

Parallelization of the exact diagonalization of the $t - t'$ -Hubbard model

W. Fettes, I. Morgenstern, T. Husslein

Universität Regensburg, Fakultät Physik, 93040 Regensburg, Germany

email: Werner.Fettes@physik.uni-regensburg.de

(29 August 1997)

Abstract

We present a new parallel algorithm for the exact diagonalization of the $t - t'$ -Hubbard model with the Lanczos-method. By invoking a new scheme of labeling the states we were able to obtain a speedup of up to four on 16 nodes of an IBM SP2 for the calculation of the ground state energy and an almost linear speedup for the calculation of the correlation functions. Using this algorithm we performed an extensive study of the influence of the next-nearest hopping parameter t' in the $t - t'$ -Hubbard model on ground state energy and the superconducting correlation functions for both attractive and repulsive interaction.

PACS: 74.20

Typeset using REVTeX

I. INTRODUCTION

The Hubbard model [1] is one of the generic models in many particle physics. Due to difficulties with the analytic solution of the Hubbard model in two dimensions, this model is intensively studied with various numerical algorithms, e.g. exact diagonalization [2], [3], [4] [5], stochastic diagonalization [6], [7] and quantum Monte Carlo algorithms [8], [9], [10], [11].

The single band Hubbard model with additional next nearest neighbor hopping is given in real the space by:

$$H = -t \sum_{\langle i,j \rangle, \sigma} c_{i,\sigma}^\dagger c_{j,\sigma} - t' \sum_{\langle\langle i,j \rangle\rangle, \sigma} c_{i,\sigma}^\dagger c_{j,\sigma} + U \sum_i n_{i,\uparrow} n_{i,\downarrow} \quad . \quad (1)$$

The sum $\langle i, j \rangle$ is over the nearest neighbors and $\langle\langle i, j \rangle\rangle$ is the sum over the next nearest neighbors. $c_{i,\sigma}^\dagger$ is the creation operator for an electron with spin σ on site i and $n_{i,\sigma}$ is the corresponding number operator. Throughout this article we take $t = 1$ as energy unit.

In the momentum space this Hamiltonian reads as:

$$H = \sum_{k,\sigma} \varepsilon_k c_{k,\sigma}^\dagger c_{k,\sigma} + U \sum_{k,p,q} c_{k,\uparrow}^\dagger c_{p,\downarrow}^\dagger c_{p-q,\downarrow} c_{k+q,\uparrow} \quad (2)$$

with

$$\varepsilon_k = -2t(\cos(k_x) + \cos(k_y)) - 4t' \cos(k_x) \cdot \cos(k_y) \quad . \quad (3)$$

The usual Hubbard-model ($t' = 0$) has a Van Hove singularity in the density of states at half filling in the noninteracting case ($U = 0$). It is possible to move this Van Hove singularity to any electron filling by extending the Hubbard model by an additional next nearest neighbor hopping t' -term in the kinetic energy. The $t - t'$ -Hubbard model [12] shows superconductivity for repulsive interactions U with $d_{x^2-y^2}$ -symmetry [11] and for attractive interaction with on site s-symmetry [13], [14], [15].

As a measure for the superconductivity we calculate the reduced two particle density matrix according to the concept of Yang [16]. From this two particle density matrix we

calculate the two particle correlation functions for different symmetries and additionally we calculate the vertex correlation function [17].

The Van Hove scenario predicts an increase of T_c for fillings close to a Van Hove singularity [18]. We study the influence of the Van Hove singularity on the superconducting correlation functions by modifying the t' -hopping parameter for fixed fillings. Here we use the Lanczos-algorithm [19], [3] as exact diagonalization technique to determine the ground state and from there ground state properties of the $t - t'$ -Hubbard model.

The basic limitations on the calculations of large system sizes with the Lanczos-algorithm is the huge memory consumption of this method. But to our surprise we found that even for Hubbard systems of size 4×4 , which the Lanczos method is capable of handling, the CPU consumption of the simulations was substantial and made a detailed scan of the parameter space given by interaction strength U , filling n and next nearest neighbor hopping t' almost impossible. We therefore implemented the Lanczos-method on IBM SP2 parallel computer with MPI (Message Passing Interface) for the communication between the processes to speed up the calculations.

II. EXACT DIAGONALIZATION WITH THE LANCZOS-ALGORITHM

Before turning our attention to the parallel techniques we outline the basic concept of the Lanczos method [19]. In the case of the exact diagonalization the Hamiltonian H of the system is written in matrix or Heisenberg representation. One chooses an orthonormal single particle basis, to represent the many-particle states. For the $t - t'$ -Hubbard model we use the momentum-space representation. Each many particle basis state $|\Phi_i\rangle$ is a product of the spin up $|\Phi_{i\uparrow,\uparrow}\rangle$ and the spin down $|\Phi_{i\downarrow,\downarrow}\rangle$ component:

$$|\Phi_i\rangle \equiv |\Phi_{i\uparrow,\uparrow}\rangle \otimes |\Phi_{i\downarrow,\downarrow}\rangle \equiv c_{k_1,\uparrow}^\dagger c_{k_2,\uparrow}^\dagger \dots c_{k_{n\uparrow},\uparrow}^\dagger \cdot c_{p_1,\downarrow}^\dagger c_{p_2,\downarrow}^\dagger \dots c_{p_{n\downarrow},\downarrow}^\dagger |0\rangle \quad , \quad (4)$$

where $c_{k_i,\sigma}^\dagger$ is the creation operator of an electron with momentum k_i and spin σ . $|0\rangle$ is the vacuum state.

Each many particle state $|\Psi\rangle$ can be represented by means of the basis states $|\Phi_i\rangle$ and coefficients α_i :

$$|\Psi\rangle = \sum_{i=1}^M \alpha_i |\Phi_i\rangle \quad . \quad (5)$$

The Hilbert space of a system consisting of a lattice of L sites and n_\uparrow electrons with spin up and n_\downarrow electrons with spin down has the dimension

$$M = M_\uparrow \cdot M_\downarrow = \binom{L}{n_\uparrow} \cdot \binom{L}{n_\downarrow} \quad . \quad (6)$$

As the size of the Hilbert space also determines the size of the computer memory, that is used in the calculation, one tries to reduce the Hilbert space. The usual way to restrict the size of the Hilbert space M is to apply symmetries of the lattice and the Hamiltonian. The translation invariance is a symmetry easily implemented when solving the $t - t'$ -Hubbard model in momentum space representation with the Lanczos algorithm. The Hilbert space decomposes into subspaces M_t^K containing only basis states $|\Phi_i\rangle$, which have the same total momentum K :

$$K = K_\uparrow + K_\downarrow = \sum_{i=1}^{n_\uparrow} k_i + \sum_{j=1}^{n_\downarrow} p_j \quad , \quad (7)$$

where k_i and p_j are the momenta of the creation operators $c_{k_i,\uparrow}^\dagger$ resp. $c_{p_j,\downarrow}^\dagger$ in eq. 4. We denote the number of states of particles with the same spin with the total momentum K_\uparrow as $M_{K_\uparrow}^\sigma$. In a 4×4 system with $n_\sigma = 4$ the number of states M_k^σ varies for different momentum between 112 and 120. The states $|\Phi_{i_\downarrow,\downarrow}\rangle$ must have the total momentum $K_\downarrow = K - K_\uparrow$, so that the product state $|\Phi_{i_\uparrow,\uparrow}\rangle \otimes |\Phi_{i_\downarrow,\downarrow}\rangle$ is in the subspace M_t^K . Altogether the subspace M_t^K has the size

$$M_t^K = \sum_{K_\uparrow=1}^L M_{K_\uparrow}^\uparrow \cdot M_{K-K_\uparrow}^\downarrow \quad . \quad (8)$$

For various fillings $n_\uparrow = n_\downarrow$ table I gives an overview.

When storing the coefficients α_i with 8 Byte floating point numbers the memory demand for one state is $8 \cdot M = 8 \cdot 4368^2 \approx 146$ MByte for a lattice with 16 sites and $n_\uparrow = n_\downarrow = 5$

electrons. Even if one uses the translation symmetry it remains a demand of $8 \cdot M_t^K \approx 9$ MByte for each state. In the standard Lanczos–algorithm [19], [20] it is necessary to store three many particle states $|\Psi\rangle$ to calculate the ground state and the ground state energy.

We implemented the Lanczos-iteration [20]:

$$\gamma_j = \langle \Psi_j | (H \cdot |\Psi_j\rangle - \beta_{j-1} |\Psi_{j-1}\rangle) \rangle \quad , \quad (9)$$

with the coefficients γ_j (diagonal) and β_j (offdiagonal) of the tridiagonal matrix T_j and the Lanczos-vectors $|\Psi_j\rangle$. From this tridiagonal matrix T_j we calculate the eigenvalues of H . In the Lanczos-scheme it is not necessary to transform the matrix H . Therefore it is even not necessary to store the matrix elements $\langle \Phi_i | H | \Phi_j \rangle$; they are only calculated, when they are needed for the further evaluation of the Lanczos-iteration (eq. 9).

III. PARALLELIZATION OF THE LANCZOS–ALGORITHM

In this section we concentrate our effort on how to speed up the simulations with the Lanczos method. The determination of the ground state properties of a Hamiltonian with the Lanczos–algorithm consists of two main parts concerning the consumption of CPU-time. First the ground state energy E_0 and the ground state $|\Psi_0\rangle$ are calculated. The second main part is the determination of the two–particle density matrix [16]:

$$\begin{aligned} \varrho_{k_1, k_2, k_3, k_4} &\equiv \langle c_{k_1, \uparrow}^\dagger c_{k_2, \downarrow}^\dagger c_{k_3, \downarrow} c_{k_4, \uparrow} \rangle \\ &= \sum_{i, j} \alpha_i \alpha_j \langle \Phi_i | c_{k_1, \uparrow}^\dagger c_{k_2, \downarrow}^\dagger c_{k_3, \downarrow} c_{k_4, \uparrow} | \Phi_j \rangle \end{aligned} \quad (10)$$

as the main observable of interest.

A. Algorithms for handling the basis states

To handle an arbitrary state $|\Psi\rangle$ it is necessary to know for each basis state $|\Phi_i\rangle$ the indices k_i and p_i of the creation operators in eq. 4 and the weights α_i .

A simple possibility for such an algorithm is the bitcoding or bitrepresentation of the basis states. Here the momenta k_i are labeled from 1 to L and the momenta p_i from $L + 1$ to $2L$. Then the states $|\Phi_i\rangle$ are expressed by an one dimensional array of bits, which are one for occupied sites, and otherwise the bits are zero. If one interprets this array as binary representation of an integer number one has an algorithm to assign each basis state $|\Phi_j\rangle$ an index j . As example we take a lattice with 4 sites and each two electrons with spin up and down:

$$|\Phi_j\rangle = c_{1,\uparrow}^\dagger c_{3,\uparrow}^\dagger \cdot c_{2,\downarrow}^\dagger c_{3,\downarrow}^\dagger |0\rangle \leftrightarrow 1010\ 0110 \leftrightarrow 166 = j \leftrightarrow \alpha_j \quad . \quad (11)$$

For any many particle state only the coefficients α_j need to be stored.

But the bitrepresentation has the great disadvantage, that a huge amount of memory is wasted, because the bitrepresentation of many integer numbers j does not correspond to a valid basis state. For a system with L latticepoints in an array of the length $(2^L)^2$ one only stores $M \ll (2^L)^2$ numbers. For the above example $L = 16$ and $n_\uparrow = n_\downarrow = 5$ there is $(2^{16})^2/M_t^K \approx 3602$.

Therefore it is desirable to use another algorithm ($|\Phi_j\rangle \leftrightarrow j$). One example is the hashing algorithm [21].

We developed a new algorithm. Though we only present results for the momentum space representation, this algorithm can also be implemented very efficiently for the exact diagonalization in real space [22].

B. Numbering of the states

First we are numbering the momenta from 1 to L ($k_i \in \{1, \dots, L\}$). Second we define $k_1 < k_2 < \dots < k_{n_\sigma}$ to fix the sign.

The state with the number 1 is

$$|\Phi_{1,\sigma}\rangle = c_{1,\sigma}^\dagger c_{2,\sigma}^\dagger \dots c_{n_\sigma,\sigma}^\dagger |0\rangle \quad . \quad (12)$$

In $|\Phi_{2,\sigma}\rangle$ the electron $c_{n_\sigma,\sigma}^\dagger$ moves from n_σ to $n_\sigma + 1$. In $|\Phi_{L-n_\sigma+1,\sigma}\rangle$ this "last" electron has reached the latticepoint L . Next in $|\Phi_{L-n_\sigma+2}\rangle$ the two creation operators with the highest index are increased by one,

$$|\Phi_{L-n_\sigma+2,\sigma}\rangle = c_{1,\sigma}^\dagger c_{2,\sigma}^\dagger \dots c_{n_\sigma-2,\sigma}^\dagger c_{n_\sigma,\sigma}^\dagger c_{n_\sigma+1,\sigma}^\dagger |0\rangle \quad . \quad (13)$$

Then the "last" creation operator moves. These are the states with the numbers $L - n_\sigma + 2$ to $2L - 2n_\sigma + 1$. Next the "last" two electrons go to the sites $n_\sigma + 1$ and $n_\sigma + 2$. If both electrons have reached the final two lattice sites ($L - 1, L$) three electrons move in the same manner through the lattice.

One gets the number i_σ of the state $|\Phi_{i_\sigma,\sigma}\rangle$ with

$$i_\sigma = \sum_{m=1}^{n_\sigma} \left(\sum_{j=l_{m-1}+1}^{l_m-1} \binom{L-j}{n_\sigma-m} \right) , \quad (14)$$

where l_m is the position of the electron m in the lattice.

Using the translational invariance of the Hamiltonian in the k-space representation means, that we keep the total momentum K of the basis states $|\Phi_i\rangle$ fixed. In this case one can only choose the "spin-up" part of the basis state free and take such a "spin-down" state, that eq. 7 is full filled. This means, we must use another convention to label the states.

We generate all states $|\Phi_{i,\sigma}\rangle$ in the sequence as described above and calculate the momentum. For each momentum we count independently the indices.

The coefficients α_i are now labeled in following way: First we combine with state number 1, momentum 1 and spin up with all possible states with spin down for a given K . Then we do the same with state number 2, momentum 1 and spin up. Next we switch to state 1 with momentum 2 and spin up and so on.

C. Dividing up the memory

In the parallel algorithm each of the P processes stores the coefficients α_i of $M_P \equiv M_t^K / P$ basis states. α_i is stored on process $p = i / M_P$.

D. Matrix-vector multiplication

In the Lanczos method it is necessary to perform a matrix-vector multiplication between the matrix H and a Lanczos-vector $|\Psi_j\rangle$. In the parallel algorithm this is carried out in the following way: For $i = 1, \dots, M_P$:

- Each process p calculates the index numbers j of the basis states $H \cdot |\Phi_{i+(p-1)M_P}\rangle$, the multiplication results for the i -th state and the process, on which the states j are stored.
- Each process exchanges the multiplication results and the numbers j of the basis states, which are not stored on the process, with process $p_j = j/M_P$.

E. Calculation of the reduced two particle density matrix

To calculate the two-particle density matrix $\varrho_{k_1, k_2, k_3, k_4}$ in an efficient way, one only calculates the elements

$$\langle \Phi_m | c_{k_1, \uparrow}^\dagger c_{k_2, \downarrow}^\dagger c_{k_3, \downarrow} c_{k_4, \uparrow} | \Phi_n \rangle \quad , \quad (15)$$

which are nonzero. That means one takes a basis state $|\Phi_n\rangle$, one of the L^4 possible combinations of k_1, k_2, k_3 and k_4 and applies $c_{k_1, \uparrow}^\dagger c_{k_2, \downarrow}^\dagger c_{k_3, \downarrow} c_{k_4, \uparrow}$ to $|\Phi_n\rangle$, afterwards one calculates the index number of this transformed basis state $|\Phi_m\rangle$.

Each process stores the complete matrix $\varrho_{k_1, k_2, k_3, k_4}$. This matrix takes for example in the 4×4 system $8 \cdot 16^4$ Byte or 512 KByte of memory.

In this algorithm one has to calculate $N_1 = M_t^K \cdot L^4$ expectation values, compared to $N_2 = (M_t^K)^2$ expectation values that would be calculated if one took all combinations $|\Phi_i\rangle$ and $|\Phi_j\rangle$ into account. In a 4×4 system with $n_\uparrow = n_\downarrow = 5$ electrons $N_2/N_1 \approx 18$ and the amount of saved CPU-time is significant. But in a 4×4 system with only $n_\uparrow = n_\downarrow = 3$ electrons $N_2/N_1 \approx 0.3$ and this algorithm is slower.

To calculate $\varrho_{k_1, k_2, k_3, k_4}$ we use a similar way for the exchange of the weights and numbers as for matrix-vector multiplication (see section III D).

At the end the values of the arrays $\varrho_{k_1, k_2, k_3, k_4}$ of all processes are summed on one process.

IV. PERFORMANCE ANALYSIS OF THE PARALLEL CODE

First we take a look on the dependence of the CPU time of one Lanczos iteration (eq. 9) for a different number of processes. As example we use a 4×4 lattice with three different numbers of electrons (fig. 1).

The small decay from 1 to 2 processes is due to communication between processes which is only necessary for more than one process. Then one sees as expected a decrease of computation time. As expected this decrease vanishes for an increasing number of processes, since the communication is growing with the number of processes.

In figure 2 we examine the CPU-consumption for the two-particle density matrix for the same system size and fillings as in figure 1. Here the gain of time is much larger than for the calculation of the energy. In this case more computation is performed for the determination of one matrix element. For more than 2 processes the dependence of nodes and CPU-time is nearly linear.

This can be understood, if we look on the numbering of the states. Most of the states $H \cdot |\Phi_i\rangle$ are stored on the same node and only for a fraction of these states the weights must be interchanged with an other process.

Summarizing the algorithm for this parallel implementation of the Lanczos-iteration and the determination of the two-particle density matrix is a coarse grained algorithm and therefore achieves a good speed-up on a parallel computer like the IBM SP2, with only some, but very powerful, processors. For very many processors the communication grows dramatically and no further speed-up is reachable.

V. NUMERICAL RESULTS

Now we want to turn our attention from the technical points of view to physical properties of the $t - t'$ -Hubbard model. Especially we study the influence of the next nearest hopping parameter t' on the ground state energy and superconducting correlation functions in the ground state of a 4×4 cluster. We focus to $n_e \equiv n_\uparrow = n_\downarrow = 5$ electrons which corresponds to a filling $\langle n \rangle = 0.625$. This is a so called closed shell situation, which can be also handled with the projector quantum Monte Carlo method [15].

First we study the ground state energy E_0 in the attractive $t - t'$ -Hubbard model (fig. 3). For small and intermediate interaction strength ($|U| \leq 10$) there is a visible difference between the energy with $t' = 0$ and $t' = -0.22$. This difference results from the changes in the structure of ε_k (eq. 3) with t' . But for large interaction strength $|U|$ the influence of the kinetic part is vanishing. In this interaction regime the ground state energy is approximately linear with U and approaches slowly the energy Un_e of the system without hopping.

Next we turn our attention to the superconducting correlation functions. In the concept of off diagonal long range order [16] the largest eigenvalue and eigenvector of $\varrho_{k_1, k_2, k_3, k_4}$ is calculated. The quantum Monte Carlo algorithms handle system sizes, where it is impossible to calculate the complete two-particle density matrix due to the memory consumptions [23]. In order to compare the exact diagonalization results with the quantum Monte Carlo data we study two-particle correlation functions for certain symmetries [24], e.g.

$$C_s(r) = \frac{1}{L} \sum_j \langle c_{j,\uparrow}^\dagger c_{j,\downarrow}^\dagger c_{j+r,\downarrow} c_{j+r,\uparrow} \rangle \quad , \quad (16)$$

$$C_d(r) = \frac{1}{L} \sum_j \sum_{\delta, \delta'} g_\delta g_{\delta'} \langle c_{j,\uparrow}^\dagger c_{j+\delta,\downarrow}^\dagger c_{j+r+\delta',\downarrow} c_{j+r,\uparrow} \rangle \quad ,$$

where the index s denotes the on site s-wave symmetry and d the $d_{x^2-y^2}$ -wave symmetry. The factor $g_\delta = \pm 1$ gives the signs of the d-wave. (+1 in x- and -1 in y-direction) These full correlation functions have nonzero values even for a system with no interaction. Responsible for this are the one-particle correlation functions

$$C_o^\sigma(r) = \frac{1}{L} \sum_j \langle c_{j,\sigma}^\dagger c_{j+r,\sigma} \rangle \quad , \quad (17)$$

which decay to zero with $\frac{1}{|r|}$ and thus do not really contribute to the long range behavior that signals superconductivity. To exclude the contribution of the one-particle correlation functions we define the vertex correlation function as

$$C_s^v(r) = C_s(r) - C_o^\uparrow(r) \cdot C_o^\downarrow(r) \quad , \quad (18)$$

$$C_d^v(r) = C_d(r) - \sum_{\delta,\delta'} (g_\delta g_{\delta'} C_o^\uparrow(r) \cdot C_o^\downarrow(r + \delta - \delta')) \quad .$$

In figure 4 we show C_s and C_s^v in dependence of the distance $|r|$. For $U = -8$ there is a visible difference only for $r = 0$. For $U = -1$ the one-particle contributions are dominant. In this case it is important to study the vertex correlation function to get the "superconducting" correlations. But already for $U = -2$ and $|r| \geq \sqrt{2}$ the difference between full and vertex correlation function is less than 30% and it is less important to take C_o^σ in account.

As a measure for the superconductivity in a system we show in fig. 5 the average of the vertex correlation function

$$\bar{C}_s^v = \frac{1}{L} \sum_i C_s^v(i) \quad . \quad (19)$$

For a small interaction strength $|U|$ the increase of the correlation functions is small. Between $U = -2$ and $U = -10$ there is a strong increase. Finally at $|U| > 10$ the curves flatten.

For correlation functions the influence of the additional hopping t' remains important even if there is nearly no difference in the energies (cp. fig. 3 and 5, $U < -10$).

Therefore we study the influence of t' for the interaction $U = -4$ (fig. 6). The correlation functions have a broad maximum around $t' = -0.50$. As it is commonly accepted [15] the finite size gap has an influence on the superconducting correlation functions. The finite size gap $g(t')$ in the energy dispersion ε_k (eq. 3) of the free system ($U = 0$) between the highest occupied state and the lowest unoccupied state is given in this case by:

$$g(t') = \begin{cases} 2 - 4 \cdot |t'| & \text{for } -0.50 \leq t' \leq 0 \\ 0 & \text{for } t' \leq -0.50 \end{cases} . \quad (20)$$

This means the finite size gap is becoming smaller with increasing $|t'|$. According to [15] this will lead to an increase in the superconducting correlations. Figure 6 confirms this for $t' > -0.50$. But at $t' < -0.50$ the correlations decrease again. Therefore also the structure of the energy dispersion ε_k has an influence on the correlation functions.

In figure 6 the maximum of the correlation functions is not at $t' = -0.37$, where the noninteracting system has a Van Hove singularity in the thermodynamic limit. There a maximum of T_c is predicted by the Van Hove scenario [18]. But for small system sizes one cannot really speak of a Van Hove singularity. Therefore the results of figure 6 are not in contradiction to the Van Hove scenario.

Yet, the question remains, whether the observed increase of the correlation function results only from a vanishing finite size gap or is related to changes of the Fermi surface. To clarify this point it will be necessary to calculate larger systems.

Next we study the influence of the t' hopping for repulsive interaction $U = 4$. Quantum Monte Carlo calculations show a plateau for the $d_{x^2-y^2}$ correlation function in the $t - t'$ -Hubbard model [24], [25]. Figure 7 shows the average correlation functions with $d_{x^2-y^2}$ symmetry.

Here the full correlation function is nearly independent of t' for $t' > -0.4$. The vertex correlation function is much smaller than in the attractive case (cp. fig. 6 and fig. 7). The increase of \bar{C}_d^v by a factor of about 10 between $t' = 0$ and $t' = -0.45$ is much larger than the increase of \bar{C}_s and \bar{C}_s^v in the attractive $t - t'$ -Hubbard model and of \bar{C}_d in the repulsive model.

In figure 8 the vertex correlation function with $d_{x^2-y^2}$ symmetry is plotted against the distance $|r|$ of the "cooper pairs". For $t' = -0.40$ the vertex correlation function has, in contrast to larger t' , no longer a negative value at $|r| = \sqrt{2}$ and is positive for all distances $|r|$. This negative value at $|r| = \sqrt{2}$ is also seen in the quantum Monte Carlo results for

larger systems [11], [26].

In the case of $t' = -0.50$, where the gap $g(t')$ gets zero, $C_d^y(|r|)$ changes its shape completely and most values are negative and also the average is negative. In contrast to the attractive $t - t'$ -Hubbard model, where the plateau is decreasing gradually, in the repulsive case one observes a complete break down of the plateau for $t' = -0.5$. This means again, that the vertex correlation function depends strongly on the energy dispersion ε_k (eq. 3), which is transformed due to the t' -hopping. As in the attractive $t - t'$ -Hubbard model the maximum of the superconducting correlations is not at $t' = -0.37$, where a Van-Hove singularity is in the non interacting infinite system.

To clarify the origin of this behavior it is necessary to study larger systems. For a possible connection with the Van-Hove-scenario it is also necessary to calculate the density of states for this parameter regime.

VI. CONCLUSION

We have presented an effective algorithm for the implementation of the exact diagonalization of the $t - t'$ -Hubbard model in momentum-space representation. As method for the exact diagonalization we use the Lanczos algorithm. We showed a detailed description of the parallel algorithm. The speed-up of the code is almost linear for the correlation functions and is increasing with increasing size of the Hilbert space.

The key point in our algorithm is a new method of labeling the states that is compact and in contrast to previous methods [21], [3] also gives a consecutive order without any interruption. This makes the distribution on the different processes for parallelization a straightforward task. With the access to powerful modern parallel computers we were able to scan the parameter space of the $t - t'$ -Hubbard model in more detail.

The influence of the t' -hopping to the ground state energy is vanishing with increasing interaction strength in the attractive $t - t'$ -Hubbard model. This is in contradiction to the correlation functions with on site s-wave symmetry, where the influence of t' is remaining

for all studied attractive interactions.

The average full and vertex on site s-wave correlation functions have a broad maximum at $t' = -0.5$, where the gap $g(t')$ is vanishing, in the attractive $t - t'$ -Hubbard model.

In the repulsive $t - t'$ -Hubbard model only the $d_{x^2-y^2}$ vertex correlation functions show a strong increase with decreasing t' and gap $g(t')$. At $t' = -0.5$ and $g(t') = 0$ \bar{C}_d^v has a break down to a negative value.

The origin of this behavior and a possible connection with the Van-Hove scenario for high T_c superconductors is yet not clear. Simulations for larger systems are necessary.

VII. ACKNOWLEDGMENT

We are grateful for the Leibnitz Rechenzentrum München (LRZ) for providing us a generous amount of CPU-time on their IBM SP2 parallel computer. Werner Fettes wants to thank the "Deutsche Forschungs Gemeinschaft" (DFG) for the financial support.

REFERENCES

- [1] J. Hubbard. *Proc. Roy. Soc.* **A276** (1963) 238.
- [2] E. Dagotto. *Phys. Rev.* **B41** (1990) 9049.
- [3] P. W. Leung and P. E. Oppenheimer. *Computers in Physics* **6** (1992) 603.
- [4] H.Q. Lin and J.E. Gubernatis. *Computers in Physics* **7** (1993) 400.
- [5] W. Fettes, I. Morgenstern, T. Husslein, H.-G. Matuttis, J.M. Singer and C. Baur, *J. Phys. I France* **5** (1995) 455.
- [6] H. De Raedt and M. Frick. *Phys. Rep.* **231** (1992) 107.
- [7] K. Michielson and H. De Raedt. *Int. J. Mod. Phys.* **B11** (1996) 1311.
- [8] S. Sorella, A. Parola, M. Parrinello and T. Tosatti. *Int. J. Mod. Phys.* **B3** (1989) 1875.
- [9] I. Morgenstern, J.M. Singer, T. Husslein and H.G. Matuttis. In *Proceedings of the 20th Int. School of Cryst.*, E. Kaldis (ed.) Kluwer, Dordrecht (1994) 331.
- [10] W. von der Linden. *Phys. Rep.* **220** (1992) 53.
- [11] T. Husslein, I. Morgenstern, D.M. Newns, P.C. Pattnaik, J.M. Singer and H.G. Matuttis. *Phys. Rev.* **B54** (1996) 16179.
- [12] D.M. Newns, P.C. Pattnaik and C.C. Tsuei. *Phys. Rev.* **B43** (1991) 3075.
- [13] R.T. Scalettar, E.Y. Loh, J.E. Gubernatis, A. Moreo, S.R. White, D.J. Scalapino, R.L. Sugar and E. Dagotto. *Phys. Rev. Lett.* **62** (1989) 1407.
- [14] E.Y. Loh (Jr.) and J.E. Gubernatis. In *Electronic Phase Transitions*, W. Hanke, Yu.V. KopaeV (ed.), North-Holland, Amsterdam (1989) 178.
- [15] D. Bormann, T. Schneider and M. Frick. *Z. Phys.* **B87** (1992) 1.
- [16] C. N. Yang. *Rev. Mod. Phys.* **34** (1962) 694.

- [17] S.R. White, D.J. Scalapino, R.L. Sugar, N.E. Bickers and R.T. Scalettar. *Phys. Rev.* **B39** (1989) 839.
- [18] D.M. Newns, C.C. Tsuei, P.C. Pattnaik and C.L. Kane. *Comments Cond. Mat. Phys.* **15** (1992) 273.
- [19] J.K. Cullum and R.A. Willoughby. *Lanczos Algorithms for Large Symmetric Eigenvalue Computations*, volume 1, 2. Birkhäuser, Boston (1985).
- [20] G.H. Golub and C.F. Van Loan. *Matrix Computations*. John Hopkins, Baltimore (1989).
- [21] E.R. Gagliano, E. Dagotto, A. Moreo and F.C. Alcarac, *Phys. Rev.* **B34** (1986) 1677.
- [22] W. Fettes. *Numerische Simulationen zu Zustandsdichten und zum Isotopeneffekt in High- T_c -Modellen*, diploma thesis, Universität Regensburg (1994).
- [23] W. Fettes, I. Morgenstern and T. Husslein. *submitted to Int. J. Mod. Phys. C* (1997).
- [24] I. Morgenstern, W. Fettes, T. Husslein, C. Baur, H.-G. Matuttis and J.M. Singer. *Proc. PC94 Conference, Lugano* (1994) 247.
- [25] S. Zhang, J. Carlson and J.E. Gubernatis. *preprint*, (1997).
- [26] T. Husslein, W. Fettes and I. Morgenstern. *Int. J. Mod. Phys. C8* (1997) 397.

TABLES

TABLE I. Size of the Hilbert space in a 4×4 system. M_σ : number of states for the electrons with spin σ , M_k^σ : number of states with spin σ and momentum k , M : size of the Hilbert space, M_t^K : size of the subspace of the Hilbert space for the states with momentum $K = (0, 0)$.

FIGURES

FIG. 1. CPU-time for one Lanczos-iteration in a 4×4 lattice.

FIG. 2. CPU-time for the determination of the two-particle density matrix $\varrho_{k_1, k_2, k_3, k_4}$ in a 4×4 lattice.

FIG. 3. Ground state energy in a 4×4 lattice with $n_\uparrow = n_\downarrow = 5$ electrons for the $t - t'$ -Hubbard model.

FIG. 4. Full ($C_s(|r|)$) and vertex correlation ($C_s^v(|r|)$) function with on site s-wave symmetry in a 4×4 lattice with $n_\uparrow = n_\downarrow = 5$ electrons in the $t - t'$ -Hubbard model with $t' = -0.22$.

FIG. 5. Average vertex correlation function (\bar{C}_s^v) with on site s-wave symmetry in a 4×4 lattice with $n_\uparrow = n_\downarrow = 5$ electrons in the $t - t'$ -Hubbard model.

FIG. 6. Average full (\bar{C}_s) and average vertex correlation (\bar{C}_s^v) function with on site s-wave symmetry in a 4×4 lattice with $n_\uparrow = n_\downarrow = 5$ electrons in the $t - t'$ -Hubbard model and the attractive interaction $U = -4$.

FIG. 7. Average full (\bar{C}_d) and average vertex correlation (\bar{C}_d^v) function with $d_{x^2-y^2}$ -wave symmetry in a 4×4 lattice with $n_\uparrow = n_\downarrow = 5$ electrons in the $t - t'$ -Hubbard model and the repulsive interaction $U = 4$.

FIG. 8. Vertex correlation ($C_d^v(|r|)$) function with $d_{x^2-y^2}$ -wave symmetry in a 4×4 lattice with $n_\uparrow = n_\downarrow = 5$ electrons in the $t - t'$ -Hubbard model and $U = 4.0$.

Parallelization of the exact diagonalization of the
 t' -Hubbard-model

W. Fettes, I. Morgenstern, Th. Hufler

June 26, 1997

Tables and Figures

Table 1

n_σ	M_σ	$\max\{M_k^\sigma\}$	M	M_t^K
1	16	1	256	16
2	120	8	14 400	912
3	560	35	313 600	19 600
4	1820	120	3 312 400	207 184
5	4368	273	19 079 424	1 192 464

Figure 1

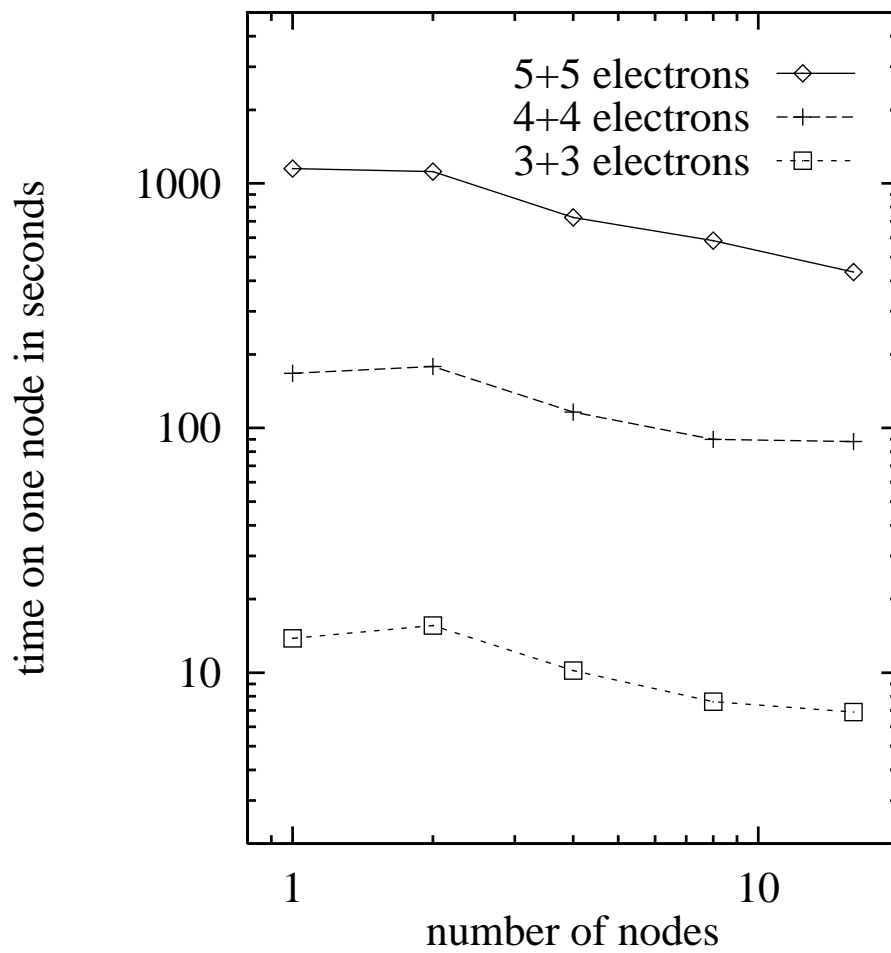


Figure 2

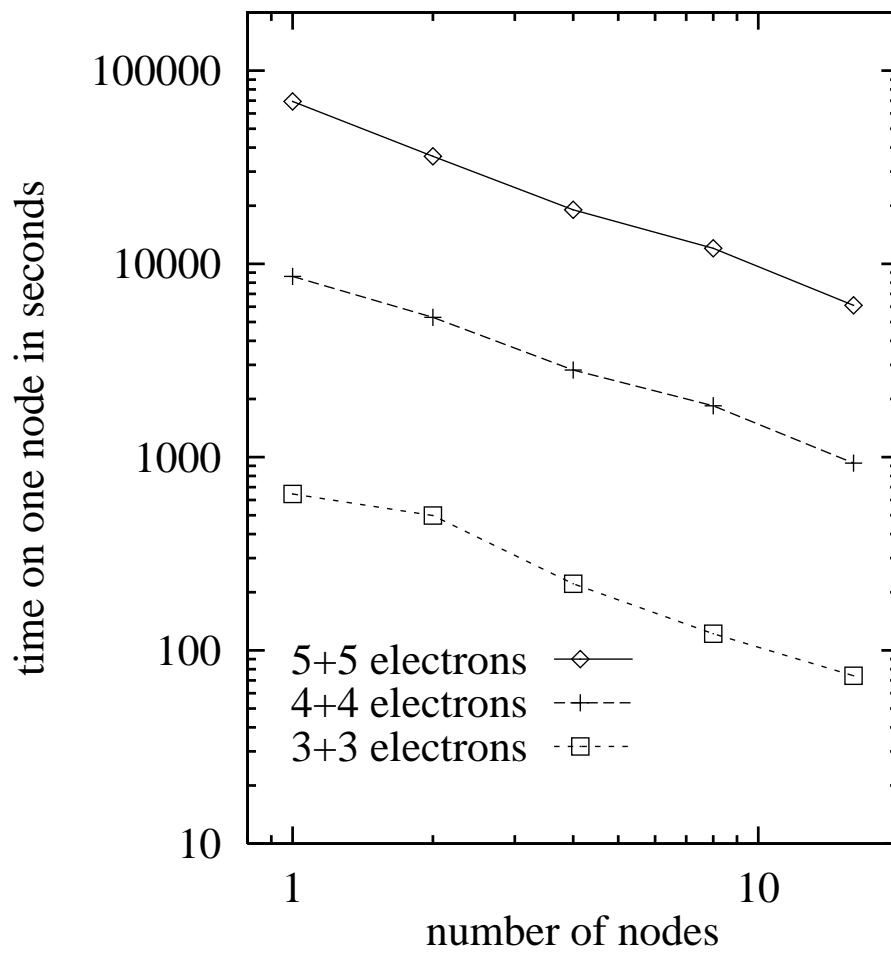


Figure 3

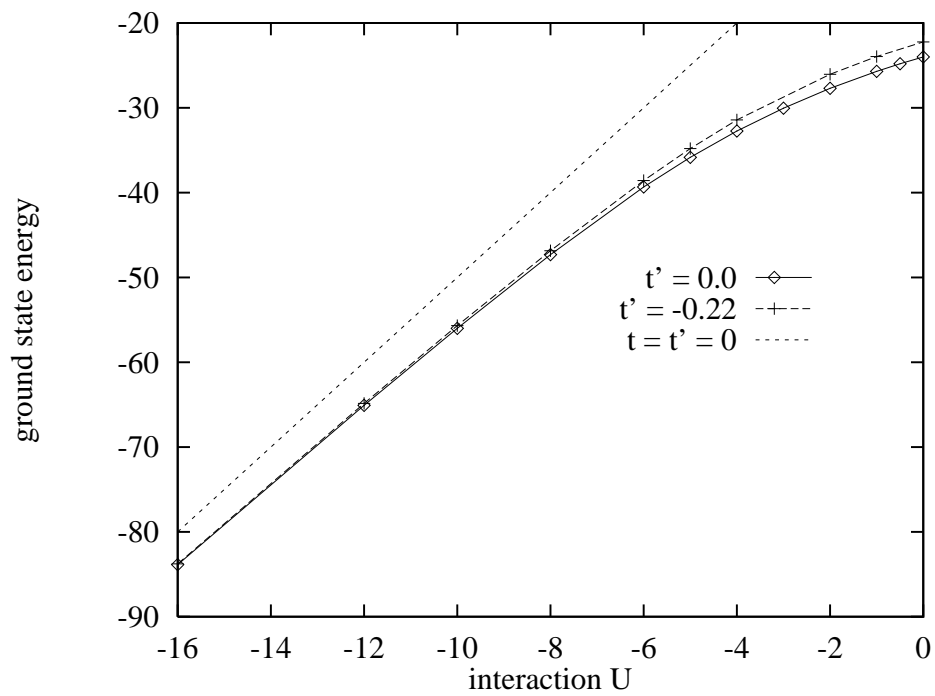


Figure 4

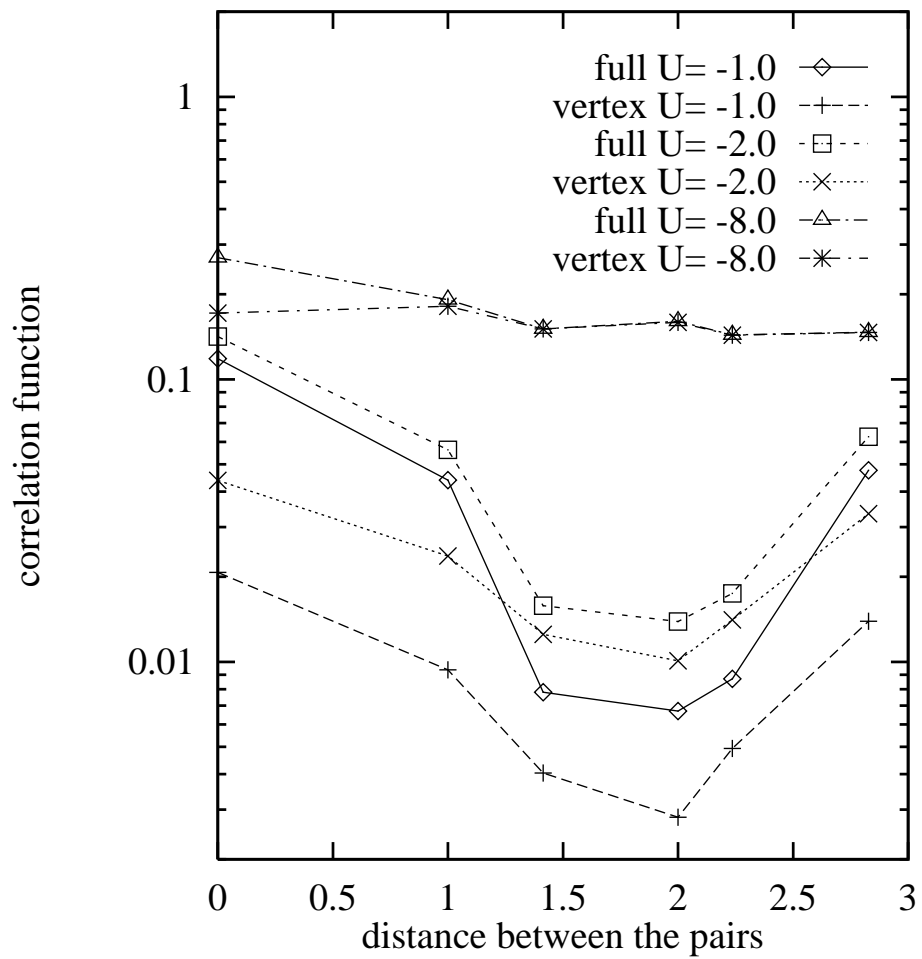


Figure 5

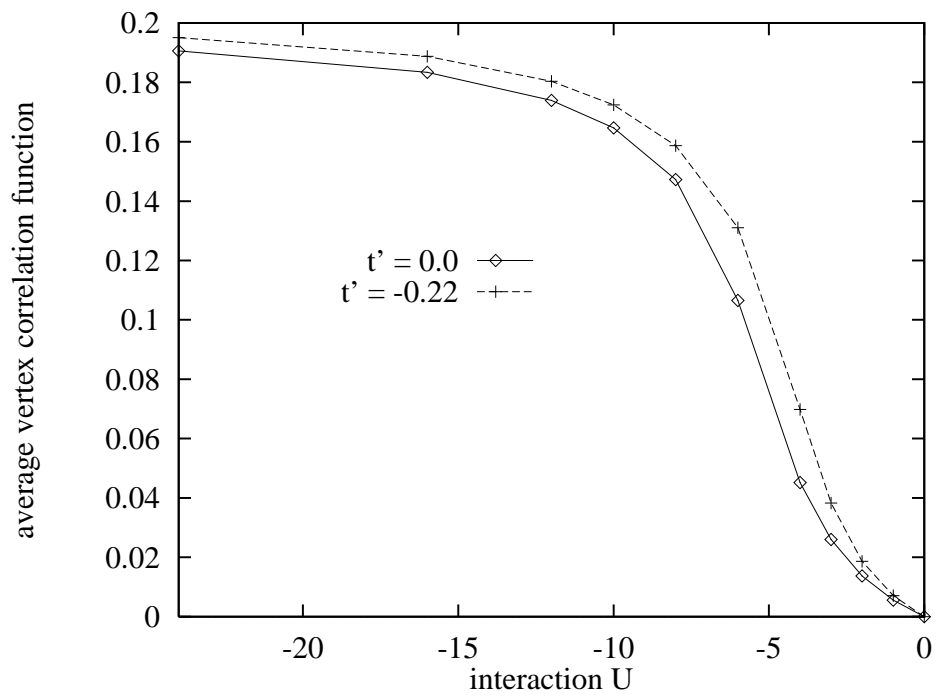


Figure 6

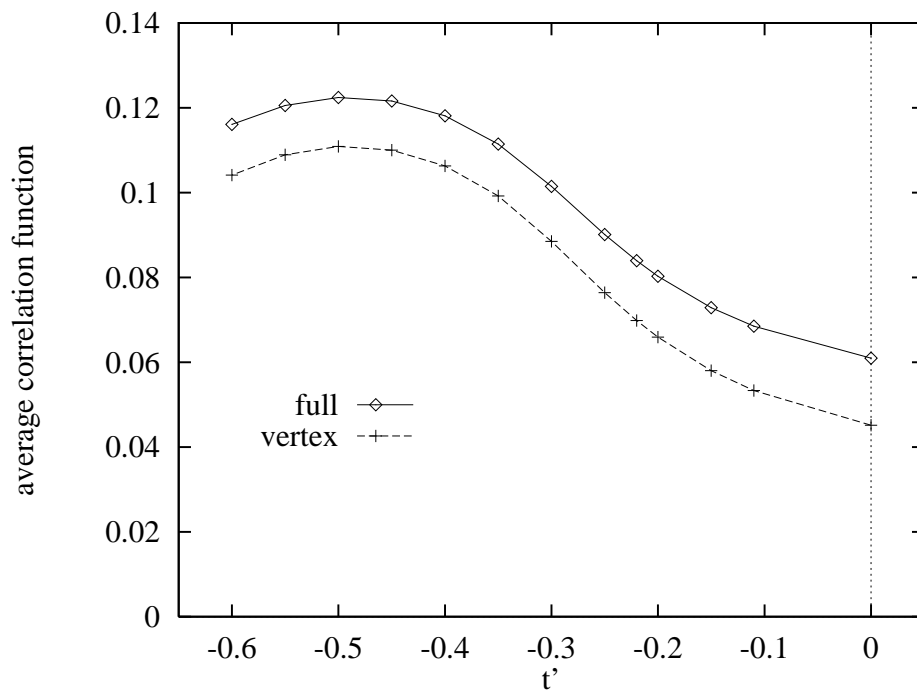


Figure 7

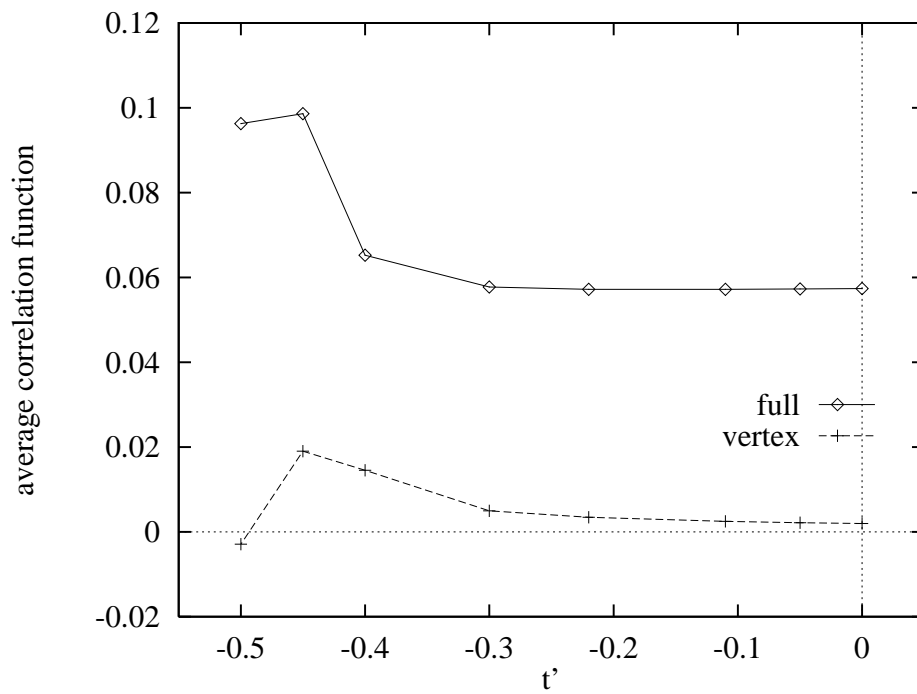


Figure 8

